

1                   **Observations on the Rheological Response of Alkali Activated Fly ash**  
2                   **Suspensions: The Role of Activator Type and Concentration**

3                   **Kirk Vance (<sup>†</sup>), Akash Dakhane (<sup>‡</sup>), Gaurav Sant (<sup>§</sup>, <sup>\*\*</sup>), Narayanan Neithalath (<sup>††\*</sup>)**

4  
5                   **ABSTRACT**

6                   This paper reports the influence of activator type and concentration on the rheological properties of alkali  
7                   activated fly ash suspensions. A thorough investigation of the rheological influences (yield stress and  
8                   plastic viscosity) of several activator parameters, including: (i) the cation type and concentration of alkali  
9                   hydroxide, and (ii) the alkali-to-binder ratio ( $n$ ) and silica modulus ( $M_s$ ), and (iii) the volume of the  
10                  activation solution, on the suspension rheology is presented. The results indicate a strong dependence on  
11                  the cation and its concentration in the activation solution. The viscosity of the activation solution and the  
12                  volumetric solution-to-powder ratio are shown to most strongly influence the plastic viscosity of the  
13                  suspension. The suspension yield stress is predominantly influenced by the changes in fly ash particle  
14                  surface charge and the ionic species in the activator. A shift from non-Newtonian to Newtonian flow  
15                  behavior is noted in the case of silicate-based suspensions for  $M_s \leq 1.5$ . This behavior, which is not  
16                  observed at higher  $M_s$  values, or when the fly ash is dispersed in hydroxide solutions or pure water, is  
17                  hypothesized to be caused by colloidal siliceous species present in this system, or surface charge effects  
18                  on the fly ash particles. Comparisons of the rheological response of alkali activated suspensions to that of  
19                  portland cement-water suspensions are also reported.

20                  **Keywords:** Geopolymer, Rheology, Fly Ash, Yield Stress, Plastic Viscosity  
21

---

<sup>†</sup> School of Sustainable Engineering and the Built Environment, Arizona State University, Tempe AZ 85287 ([kevince@asu.edu](mailto:kevince@asu.edu))

<sup>‡</sup> School of Sustainable Engineering and the Built Environment, Arizona State University, Tempe AZ 85287 ([adakahne@asu.edu](mailto:adakahne@asu.edu))

<sup>§</sup> Department of Civil and Environmental Engineering, University of California Los Angeles, Los Angeles, CA, [gsant@ucla.edu](mailto:gsant@ucla.edu)

<sup>\*\*</sup> California Nanosystems Institute,, University of California Los Angeles, Los Angeles, CA

<sup>††\*</sup> School of Sustainable Engineering and the Built Environment, Arizona State University, Tempe AZ 85287  
([Narayanan.Neithalath@asu.edu](mailto:Narayanan.Neithalath@asu.edu)); Corresponding Author. Phone: 001-480-965-6023; Fax: 001-480-965-0557

22 **NOMENCLATURE**

$n$	ratio of $\text{Na}_2\text{O}$ in the activator to the total fly ash content
$M_s$	ratio of $\text{SiO}_2$ -to- $\text{Na}_2\text{O}$ in the activator
$(a_s/p)_v$	Activation solution-to-powder ratio, by volume (Refer to the definition of activation solution in 2.1)
$(a_s/b)_v$	Activation solution-to-binder ratio, by volume; binder implying fly ash here
$(w/s)_m$	Water-to-solids ratio, mass-based (Refer to the definition of solids in 2.1)
$w/c$	Water-to-cement ratio, mass-based, for OPC systems
$\tau$	Shear stress, Pa
$\tau_y$	Yield stress, Pa
$\eta_p$	Plastic viscosity, Pa.s
$\eta_a$	Apparent viscosity, Pa.s
$\dot{\gamma}$	Shear rate, $\text{s}^{-1}$

23

## 24 1.0 INTRODUCTION

25 Ordinary portland cement (OPC) based concrete is one of the most widely used materials globally, and  
26 production of OPC has been shown to require a significant quantity of energy and release significant  
27 quantities of CO<sub>2</sub>. One of the sustainable alternatives to OPC that has been gaining attention is the use of  
28 geopolymeric or alkali activated materials, where alumino-siliceous wastes/by-products such as fly ash or  
29 slag can be activated using alkalis to create a binding medium that is X-ray amorphous and has a three-  
30 dimensional network structure (Palomo et al. 1999; Puertas and Fernández-Jiménez 2003; Škvára et al.  
31 2009). The formation of the binding gel is a complex process including the dissolution process where Si  
32 and Al from the source materials are dissolved into a highly alkaline solution, precipitation of  
33 aluminosilicate gel, and further polymerization and condensation to develop the final microstructure  
34 (Davidovits 1999; Davidovits 2005). Geopolymeric systems are reported to demonstrate similar or  
35 superior mechanical and durability properties compared to OPC-based concretes (Bijen 1996; Fernández-  
36 Jiménez et al. 2007; Bernal et al. 2012). Geopolymers based on coal fly ash are of particular interest  
37 because of the potential utilization of a waste material that is available in large quantities as well as the  
38 beneficial properties of the resulting binder (Provis et al. 2007).

39 While several studies have examined the mechanical/durability properties of fly ash-based geopolymers,  
40 there have been very few studies on aspects related to their rheological response. A few studies have  
41 investigated the flow behavior of fly ash-based geopolymers using conventional concrete workability  
42 techniques (Qing-Hua and Sarkar 1994; Poulesquen et al. 2013) and investigated the influence of  
43 superplasticizing admixtures on the rheology of these systems (Termkhajornkit and Nawa 2004; Criado et  
44 al. 2009; Palacios et al. 2009; Burgos-Montes et al. 2012). Superplasticizers are superfluidificants which  
45 are typically composed of polar chain polymers which act as both deflocculant and suspension stabilizer  
46 (Pasquino et al. 2013). The charged polymers adsorb on the surface of cement grains acting to disperse  
47 cement particles and breakup agglomerations, freeing water in the suspension and enhancing flowability  
48 while enhancing the stability of the particles in suspension (Cyr et al. 2000; Papo and Piani 2004; Mikanovic  
49 and Jolicoeur 2008). Studies on the influence of superplasticizers on the flowability of geopolymer  
50 suspensions have generally found mixed results (Criado et al. 2009; Palacios et al. 2009), indicating that  
51 the nature of these suspensions is likely different from that of OPC suspensions.

52 This paper aims to build improved understanding of the rheology of fly ash activated geopolymers and  
53 explore the influence of activator type and composition on their rheological properties. Two different  
54 classes of activators are used in this study where Class F fly ash is used as the principal solid precursor: (i)

55 sodium or potassium hydroxide, and (ii) sodium or potassium silicate, whose solutions in water are  
 56 conditioned to different  $\text{SiO}_2\text{-M}_2\text{O}$  ratios ( $M_s$ ) and  $\text{M}_2\text{O}$ -to-fly ash powder ratios ( $n$ ), where  $M$  is the cation.  
 57 The rheological parameters considered are the yield stress and plastic viscosity of the suspensions  
 58 determined using the well-known Bingham model. Obtaining a detailed understanding of the rheological  
 59 influences of alkali cation type and activation solution viscosity is emphasized. Additionally an in-depth  
 60 investigation of the rheology is attempted using a *wide shear range* method as illustrated in (Vance, Kirk  
 61 2014), where model-less estimations of rheological parameters are achieved. This experimental approach  
 62 is used to compare the rheological nature of these suspensions to those of OPC-water suspensions.  
 63 Limited shear stress growth rheological studies are described in an effort to discern the transition between  
 64 Newtonian and non-Newtonian behaviors with changing silicate activator chemistry.

65 **2.0 EXPERIMENTAL PROGRAM**

66 **2.1 Experimental Parameters**

67 A Class F fly ash conforming to ASTM C 618 (2013) was used as a solid precursor. The chemical composition  
 68 of fly ash as determined using x-ray fluorescence (XRF) is shown in Table 1; the residual quantity  
 69 represents the impurities and other compounds which cannot be identified through XRF. The specific  
 70 surface area (SSA) of fly ash was measured to be  $218 \text{ m}^2/\text{kg}$  using Blaine’s air permeability apparatus. The  
 71 median particle size, measured using the dynamic light scattering method was  $19.9 \mu\text{m}$ . The loss on  
 72 ignition (LOI) of the fly ash is determined by measuring the mass loss of the fly ash powder between  $105^\circ\text{C}$   
 73 and  $1000^\circ\text{C}$ .

74 Table 1: Chemical composition and physical properties of fly ash

$\text{SiO}_2$	$\text{Al}_2\text{O}_3$	$\text{Fe}_2\text{O}_3$	$\text{CaO}$	$\text{MgO}$	$\text{SO}_3$	$\text{Na}_2\text{O}$	$\text{K}_2\text{O}$	LOI	SSA
58.4%	23.8%	4.19%	7.32%	1.11%	0.44%	1.43%	1.02%	0.5%	$218 \text{ m}^2/\text{kg}$

75 The activators used were hydroxide or silicate solutions of Na or K. The concentration of NaOH and KOH  
 76 solutions used was 4M and 8M. The activation solution refers to the solution of water and the alkali salt(s):  
 77 alkali hydroxide and/or alkali silicates in which the fly ash is suspended. When silicate-based activators  
 78 are used, this includes the solids content in the activator solution, the water content in the activator  
 79 solution, and the additional water required to obtain the desired water-to-powder ratio. In other words,  
 80 i.e., the activation solution is the suspending fluid. The activation solution-to-fly ash ratio (mass-basis)  
 81 used was 0.35 corresponding to a volumetric ratio of activation solution-to-powder  $(a_s/p)_v$  of between  
 82 0.85 and 0.90. The Na- and K-silicate solutions for activation were proportioned considering two  
 83 parameters: (i)  $n$  – the ratio of  $\text{Na}_2\text{O}$  in the activator to the total fly ash content; and (ii)  $M_s$  – the ratio of

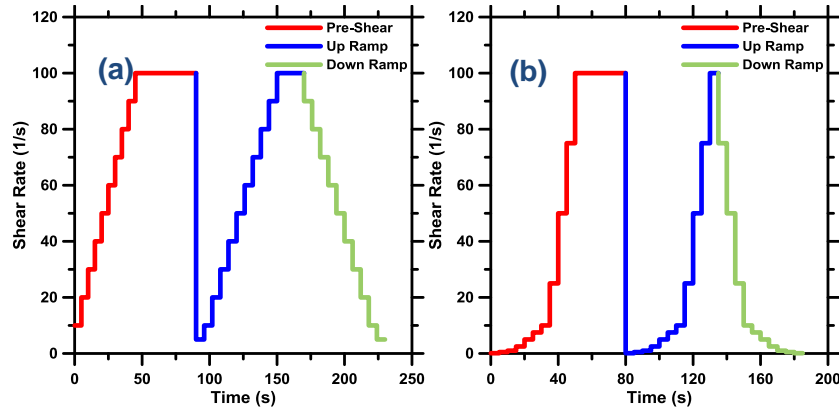
84 SiO<sub>2</sub>-to-Na<sub>2</sub>O in the activator. Two different n values were used: 0.03 and 0.05. The mass-based M<sub>s</sub> values  
85 of the as-obtained Na- and K-silicates were 3.22 and 2.10 respectively, which corresponds to mole-based  
86 values of 3.32 and 3.29. The solids content in the silicate solutions was approximately 36%. Requisite  
87 amounts of NaOH or KOH were added to the silicate solutions to adjust the M<sub>s</sub> (mole-based) to 2.5 or 1.5  
88 for both Na- and K-silicate solutions. M<sub>s</sub> values in this range have been shown to be necessary to induce  
89 sufficient activation and strength development (Ravikumar and Neithalath 2012b; Ravikumar and  
90 Neithalath 2012a). For the Na- and K-silicate activated fly ashes, the mass-based water-to-solids ratio -  
91 (w/s)<sub>m</sub> - used was 0.20 and 0.25 which corresponds to a (a<sub>s</sub>/ρ)<sub>v</sub> between 0.59 and 0.74 and between 0.72  
92 and 0.88 respectively. The solids in (w/s)<sub>m</sub> consists of fly ash, the solid fraction of the K- or Na-silicate  
93 activator, and the solid fraction of the alkali hydroxide used to adjust the M<sub>s</sub>, and the liquid consists of the  
94 water in the activator solution and the water added to achieve at the desired (w/s)<sub>m</sub>. In order to facilitate  
95 comparisons between the rheological performances of these suspensions, it may be necessary to consider  
96 the solid loading on a volume basis. Hence in the discussion section, the actual volume-based activation  
97 solution-to-powder ratios - (a<sub>s</sub>/ρ)<sub>v</sub> for the corresponding (w/s)<sub>m</sub> are used. An OPC suspension  
98 proportioned at a mass-based water-to-cement ratio (w/c) of 0.45 (which corresponds to a w/c of 1.42  
99 on a volume-basis), was also proportioned so as to provide a point of comparison of fly ash geopolymer  
100 rheology to those of commonly used OPC systems.

## 101 **2.2 Mixing and Testing Procedure**

102 Liquid activators were prepared prior to mixing with the binder (fly ash), and allowed to cool down for a  
103 period of 3 to 4 hours to ambient temperature (22±2°C) as measured with an infrared thermometer. For  
104 the rheological studies of activation solutions, approximately 12 mL of solution was placed using a  
105 disposable syringe in a TA Instruments AR2000EX rheometer in the concentric cylinder configuration, in  
106 which both the cup and bob were textured, to reduce slip. The gap between the concentric cylinders was  
107 fixed at 1.0 mm. For studies of fresh geopolymer suspensions, approximately 200 g of the suspension was  
108 mixed using a kitchen blender as follows: (1) initial hand mixing to disperse the powder in the activation  
109 solution and to ensure that particles do not adhere to the edges of mixing container, (2) mixing in the  
110 blender at high speed for 30s, (3) 30s covered rest period, and (4) final mixing at high speed in the blender  
111 for 30s. This mixing sequence is a modification to ASTM C1738 (2011) which provides recommendations  
112 for measurements of cement paste rheology (Nehdi and Rahman 2004); but has been demonstrated to  
113 provide similar fluidity and mixing consistency. After mixing, approximately 6 mL of sample was extracted  
114 using a disposable syringe and placed in the rheometer in the parallel plate configuration. The gap

115 between the top and bottom plates parallel plates (top plate diameter of 50 mm, serrated to a depth of  
116 1.0 mm) was set to 2.0 mm during the experiments, as this gap has been noted to provide consistent  
117 results in cementitious suspensions (Vance, Kirk 2014). The bottom plate was serrated to a depth of 0.15  
118 mm. Shearing surfaces were serrated to minimize the effects of slip and localized particle migration from  
119 the shearing surface (Mannheimer 1983; Saak et al. 2001). Shearing surfaces were serrated to different  
120 depths to avoid the serrations of the upper and lower geometries from keying into each other, resulting  
121 in an incorrect gap as well as potentially damaging the rheometer. The rheological studies were carried  
122 out with the Peltier plate set to a temperature of  $25\pm 0.1$  °C. The approximate time from the addition of  
123 the activation solution to the start of the rheological experiment was 150 s. Treatment and conditioning  
124 of experimental data was carried out for shear stress and shear rates using the TA Instruments TRIOS  
125 software package. For all rheological experiments, three replicate suspensions were generated and  
126 studied, and experimental duration was set to minimize potential effects of sedimentation.

127 The general experimental procedure consists of varying the shear rate as follows: (1) a stepped ramp-up  
128 pre-shear phase, (2) a subsequent stepped ramp-up, and (3) a stepped ramp-down phase. The actual data  
129 acquisition is carried out during steps (2) and (3). Shear stress values are recorded every second, with a  
130 given shear step being terminated when a steady state has been achieved, as defined by 3 consecutive  
131 measurements within 5% of each other. For all the studies, the values used in determining rheological  
132 properties are the steady state values of shear stress and the related shear rate in the down ramp. Two  
133 different rheological evaluations are conducted. The shear rate range used for the studies of activation  
134 solutions and the suspension was 5-to-100/s, hereinafter referred to as the “normal” shear rate range.  
135 This is the shear rate range that is used in a majority of rheological studies on cementitious suspensions  
136 (Nehdi and Rahman 2004; Banfill 2006). For the comparative study of geopolymers and cementitious  
137 suspensions, a “wide” shear rate range: 0.005-to-100/s was used. The “wide” experiment follows a recent  
138 study (Vance, Kirk 2014) in an effort to characterize and adequately model the stress plateau which only  
139 manifests are very lower shear rates (Barnes 1999). A graphical representation of the two rheological  
140 procedures used in this study is presented in Figure 2. In addition, an oscillatory shear stress growth study  
141 was carried out to investigate the unexpected Newtonian behavior when an activation solution with a  
142 low(er)  $M_s$  was used. Here, a coaxial cylinder geometry was used with an oscillatory frequency of 1 Hz and  
143 a stress range from 0.005 Pa to 50 Pa was employed. Stress ranges below 0.1 Pa resulted in torque  
144 readings that were close to the torque limit of the instrument, resulting in significant data scatter and  
145 thus such data is disregarded in the analysis.



146

147

**Fig. 1** Rheological procedure: (a) “normal” shear range and (b) “wide” shear range

148

149

150

151

152

153

154

The viscosity of the activation solutions was determined by fitting the rheological data to the Newtonian flow model shown in Equation 1. The rheological model parameters for the “normal” shear rate range (5- to-100/s) for geopolymers suspensions was calculated by fitting the down-ramp data to the Bingham model shown in Equation 2 (Bingham 1922). The use of Bingham and Newtonian models and their adequacy (or lack thereof) is better considered by analysis of additional data provided via “wide” shear rate range studies. In the equations below,  $\tau$  is the shear stress (Pa),  $\tau_y$  is the yield stress (Pa),  $\eta_p$  is the plastic viscosity (Pa.s), and  $\dot{\gamma}$  is the shear rate ( $s^{-1}$ ).

155

Newtonian: 
$$\tau = \eta_a \dot{\gamma} \quad \text{Equation (1)}$$

156

Bingham: 
$$\tau = \tau_y + \eta_p \dot{\gamma} \quad \text{Equation (2)}$$

157

### 158 3.0 RESULTS AND DISCUSSIONS

159

160

161

162

This section discusses the influence of the type and chemistry of the alkaline activation solution on the rheological parameters of fly ash suspensions determined using the Bingham model. The solution is also evaluated in itself to account for the influences of ion concentrations on solution viscosity, which in turn influences the rheological properties of the suspension.

163

#### 163 3.1 Rheological Behavior of the Activation Solutions

164

165

166

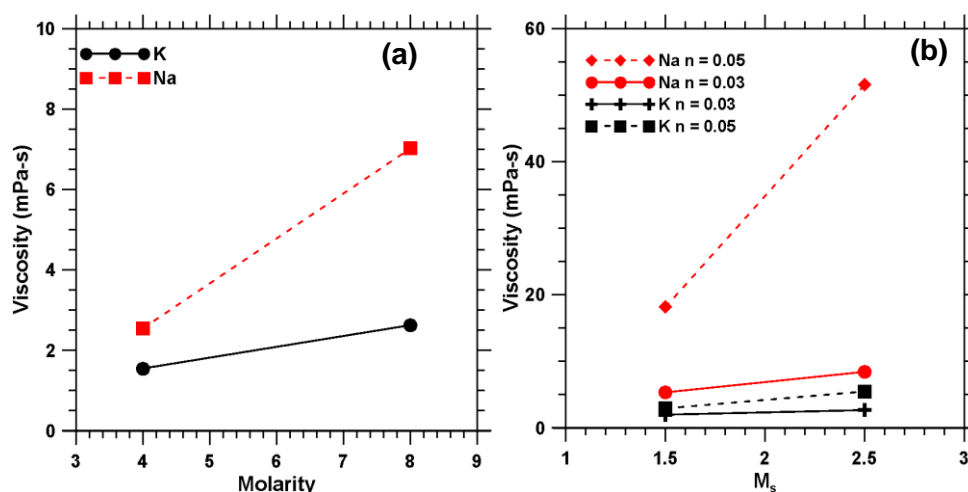
167

The rheology of the activation solutions was evaluated in the “normal” shear rate range (5-to-100/s). 4M and 8M NaOH and KOH solutions were used to explore the influence of concentration and cation type on flow properties. Additional experiments were carried out using Na-and-K- silicate solutions to investigate the influence of n,  $M_s$  and cation type on solution rheology, and for comparison with hydroxide solutions.

168 Expectedly, all of the activation solutions demonstrated Newtonian behavior over the range of shear rates  
169 investigated.

170 The influences of alkali cation, molarity, and  $n$  and  $M_s$ , respectively on the solution viscosity are presented  
171 in Figures 2(a-b). For reference, the viscosity of water at 25°C is approximately  $8.9 \times 10^{-4}$  Pa.s. Na-  
172 containing solutions demonstrate higher viscosities than the K-containing ones over all values of  $n$  and  $M_s$   
173 considered, which is in line with reports in the literature (Provis and Van Deventer 2009). The error was  
174 determined to be less than 2% on replicate measurements for the activation solutions and less than 5%  
175 for the alkali activated fly ash pastes on replicate measurements.

176



177

178 **Fig. 2** Influence of: (a) molarity of KOH and NaOH solutions on its viscosity, and (b)  $n$ ,  $M_s$  of K-silicate and  
179 Na-silicate activators on its viscosity. The viscosities were extracted using a Newtonian model.

180 From Figure 2(a) two obvious trends emerge: increasing concentration increases the solution viscosity  
181 regardless of the cation type, and Na-based activators result in significantly higher viscosities compared  
182 to K-based activators, at equivalent concentrations. As an example: at a concentration of 8 mol/L, the  
183 viscosity of the NaOH solution is 3 times higher than the corresponding KOH solution. The viscosity of  
184 aqueous solutions is described by ion-ion interactions and ion-dipole forces. As the ionic concentration  
185 increases, the influence of ion-dipole forces increases, resulting in an increase in the measured viscosity.  
186 The higher charge density of  $\text{Na}^+$  ions results in higher ion-dipole forces in the NaOH solution, thereby  
187 increasing their viscosity relative to the KOH solution.

188 When silicate bearing activators are used, a similar trend with respect to the alkali cation is noted (Figure  
189 2b). In addition, a general increase in viscosity with increasing  $M_s$  and  $n$  is observed, with the effect once  
190 again being more noticeable for the Na cation than for K. NMR studies of concentrated alkali silicate

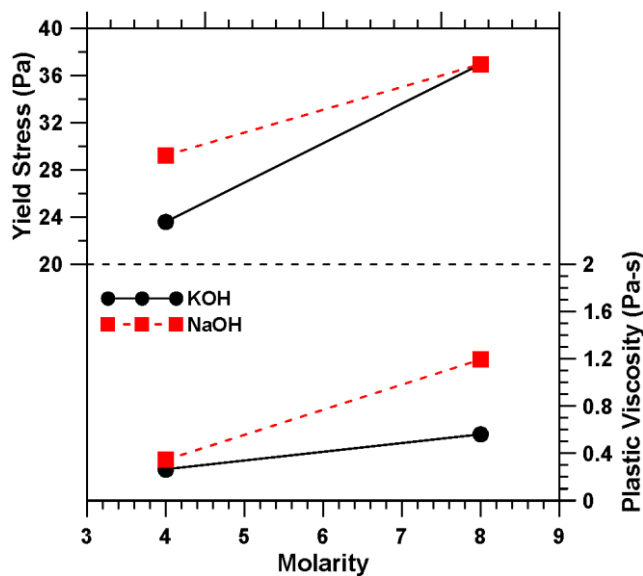


191 solutions have indicated the presence of colloidal Si-O-H-M complexes (where M denotes Na or K species)  
192 on the order of 0.6 nm in size, which form aggregates on the order of a few nm (Stebbins et al. 1992;  
193 Tognonvi et al. 2010), the presence of which increases the solution viscosity (Brady 1993). The  
194 quantity/size of these colloidal species and aggregates likely increases with  $M_s$  due to an increased Si (i.e.,  
195 complex) content and the reduced abundance of  $\text{OH}^-$  species to break Si-O-Si bonds (Iler 1979), which  
196 results in an increase in the solution viscosity (Svensson et al. 1986; Wijnen et al. 1989). On the other  
197 hand, an increase in  $n$  increases the ionic concentration of Na or K, and Si species in the solution, resulting  
198 in increased ion-dipole forces and an increased quantity of Si-O-H-M complexes. In addition, to obtain  
199 identical  $n$  and  $M_s$  values for Na and K silicate solutions, more Na-silicate is needed (than K-Silicate) due  
200 to the lower molecular weight of sodium. This results in inequivalent ion-dipole forces in these solutions,  
201 as a result of which Na-bearing silicate solution show higher viscosities. Figure 2(b) also shows that, with  
202 an increasing value of  $n$ , the viscosity enhancement is higher with increasing  $M_s$  when  $\text{Na}^+$  is the cation in  
203 solution. This behavior is attributed to the more significant influence of ion-dipole forces with smaller,  
204 more charge dense  $\text{Na}^+$  ions combined with higher colloidal species concentration.

### 205 **3.2 Rheological Behavior of Fly Ash Suspensions Activated with NaOH or KOH**

206 Rheological studies were performed on suspensions where fly ash was dispersed in NaOH or KOH solutions  
207 (4M and 8M) using the “normal” shear rate range protocol described in Section 2. From Figure 3 it is  
208 observed that increasing the activation solution concentration results in an increase in the plastic viscosity  
209 and yield stress of the suspensions. This behavior is primarily attributed to the increase in the viscosity of  
210 the activation solution with concentration. Similarly, the effect of the cation on the rheological  
211 performance of the suspension can also be related to the rheology of the medium in which the fly ash is  
212 dispersed. As seen in Figure 2(a), NaOH solutions demonstrate higher viscosity than the KOH solutions.  
213 The change in plastic viscosity of the fly ash-NaOH suspension as compared to the fly ash-KOH suspension  
214 when the concentration increases also mimics trends in the viscosity of the activation solution. Yield  
215 stress, however, increases at a greater rate with an increase in activation solution concentration when  
216 the fly ash is dispersed in KOH. At low(er) concentrations, the yield stress of the fly ash-NaOH suspension  
217 is higher than that of the fly ash-KOH suspension, while at higher concentrations, the yield stress values  
218 of the two suspensions are similar. The yield stress of a suspension is influenced by several competing  
219 effects: (i) the viscosity of the fluid, (ii) interparticle forces (interaction potential or steric forces and van  
220 der Waals forces), and (iii) the influence of particle jamming (Barnes 1999; Lowke 2009). As the volume  
221 fraction of solids (fly ash) is similar for all these mixtures and the fly ash particles are spherical, the

222 influence of particle jamming can be ignored in comparative evaluations. Similarly, particle spacing also  
 223 will be approximately similar across these suspensions, and thus the influence of van Der Waals forces is  
 224 likely redundant. The yield stress can be considered to be proportional to the inverse square of particle  
 225 separation (van der Waals forces) minus the square of the interaction potential (zeta potential) (Scales et  
 226 al. 1998). Increased particle separation will decrease the effect of van Der Waals forces, while a higher  
 227 net surface charge on the particles will increase the repulsive force between particles, both effects  
 228 resulting in a decrease in yield stress. This behavior can be conceptually verified by considering the surface  
 229 interaction effect that results from the use of superplasticizers in cementitious suspensions (Papo and  
 230 Piani 2004). As such, there remain two influences which may explain the relative increase in yield stress  
 231 with increasing molarity: interaction potential and viscosity of the activation solution. Studies have shown  
 232 the zeta-potential of fly ash is dependent on ion type, ion concentration and the pH of the suspending  
 233 solution (Nägele 1986; Nägele and Schneider 1989). In solutions of NaOH and KOH, the zeta potential of  
 234 fly ash has been shown to be negative, with those in NaOH solutions showing a larger negative potential  
 235 (Nägele and Schneider 1989). This behavior is attributed to the enhanced adsorption of  $K^+$  on the fly ash  
 236 particle surfaces than  $Na^+$  ions (Franks 2002), resulting in a less negative surface charge as the  $K^+$   
 237 concentration is increased. As the zeta potential decreases (i.e., becomes less negative), the yield stress  
 238 increases due to a decreased repulsive force between fly ash particles. The smaller increase in yield stress  
 239 in NaOH solutions as compared to KOH solutions with increasing molarity can thus be attributed to the  
 240 greater negative surface charge of fly ash particles in NaOH that result in more significant repulsive forces.



241

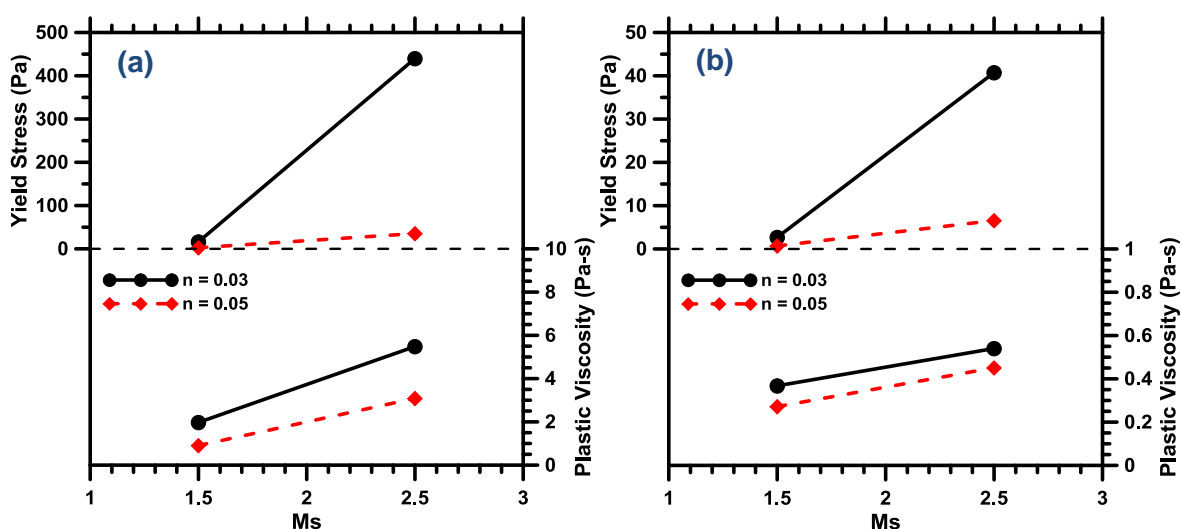
242 **Fig. 3** Influence of molarity of KOH and NaOH on the rheological properties determined using the  
 243 Bingham model

### 244 3.3 Rheological Behavior of Fly Ash Suspensions Activated using Na- or K-Silicates

245 The following discussions highlight the major factors influencing the rheological parameters of fly ash  
246 suspensions activated using Na- or K-silicate solutions. Two key factors are identified and explored: (i) the  
247 viscosity of the suspending media as dictated by the  $M_s$  of the activator and  $n$  of the suspension, and (ii)  
248 the volume of activation solution present.

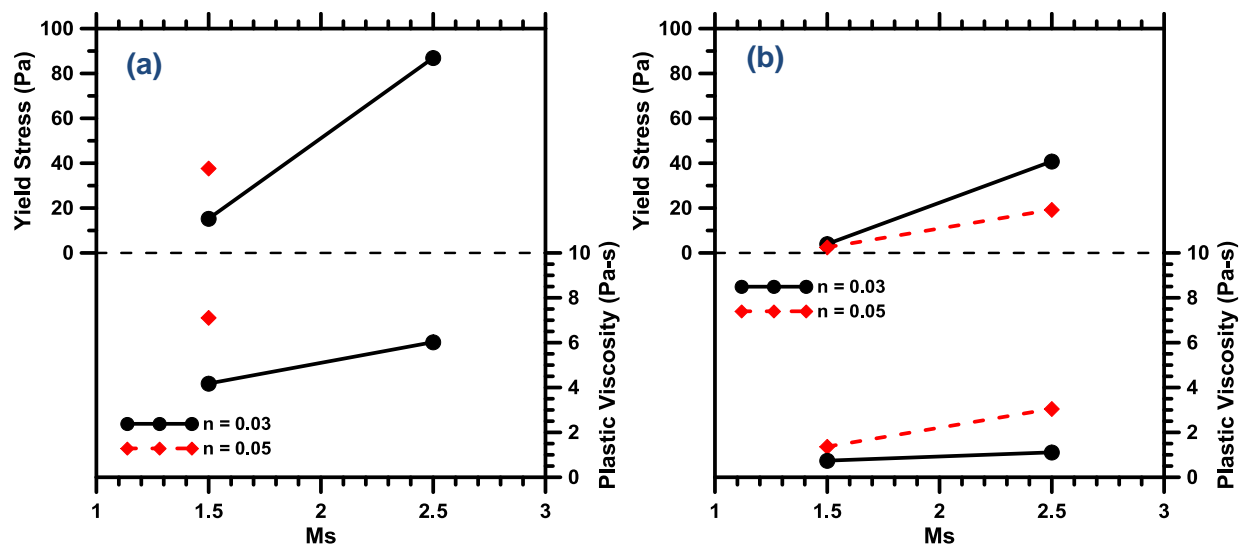
#### 249 3.3.1 Influence of $n$ , $M_s$ and $(w/s)_m$

250 Rheological studies were performed on suspensions where fly ash was dispersed in Na- or K-silicate  
251 solutions. For the silicate based activators, MOH was added to reduce the  $M_s$  of the as-obtained silicate  
252 solutions to the desired values (1.5 and 2.5 in this study). The rheological studies were performed using  
253 the “normal” shear rate range as described in Section 2. Figures 5 and 6 show the influence of  $n$  and  $M_s$   
254 on the yield stress and plastic viscosity of fly ash-K silicate and fly ash-Na silicate suspensions respectively  
255 for two different  $(w/s)_m$  – 0.20 (Figures 4(a) and 5(a)) and 0.25 (Figures 4(b) and 5(b)) corresponding to  
256  $(w/s)_v$  ratios of between 0.57 and 0.74 and between 0.72 and 0.88 for  $(w/s)_m$  ratios of 0.20 and 0.25  
257 respectively. For the Na-silicate activated case, a suspension at a  $(w/s)_m$  of 0.20 could not be proportioned  
258 with an  $n$ -value of 0.05 and  $M_s$  of 2.5 because the water from the silicate activators themselves produced  
259 a  $(w/s)_m$  higher than 0.20. Increasing the  $(w/s)_m$  from 0.20 to 0.25 results in a drastic decrease in the yield  
260 stress and plastic viscosity as would be expected. Increasing the amount of suspending fluid in a  
261 suspension increases the particle spacing, thereby increasing the fluid film thickness around the particles,  
262 thus decreasing yield stress and plastic viscosity. Increasing the water content also reduces the alkali ion  
263 concentration in the solution which reduces the viscosity of the activation solution, further contributing  
264 to a decrease in the values of the rheological parameters.



265

266 **Fig. 4** Influence of  $M_s$  on the rheological properties of fly ash-K silicate suspensions determined using the  
 267 Bingham model for: (a) 0.20  $(w/s)_m$  and (b) 0.25  $(w/s)_m$ . Note the difference in the ranges of yield stress  
 268 and plastic viscosity with changing  $(w/s)_m$ . The Y-axis scales are different in both these graphs.



269

270 **Fig. 5** Influence of  $M_s$  on the rheological properties of fly ash-Na silicate suspensions determined using  
 271 the Bingham model for: (a) 0.20  $(w/s)_m$  and (b) 0.25  $(w/s)_m$ . At a  $(w/s)_m$  of 0.20, a fly ash-Na silicate  
 272 suspension with an  $M_s$  of 2.5 and  $n$  of 0.05 was not possible because it would have meant removing  
 273 water from the activators to obtain the desired  $(w/s)_m$ .

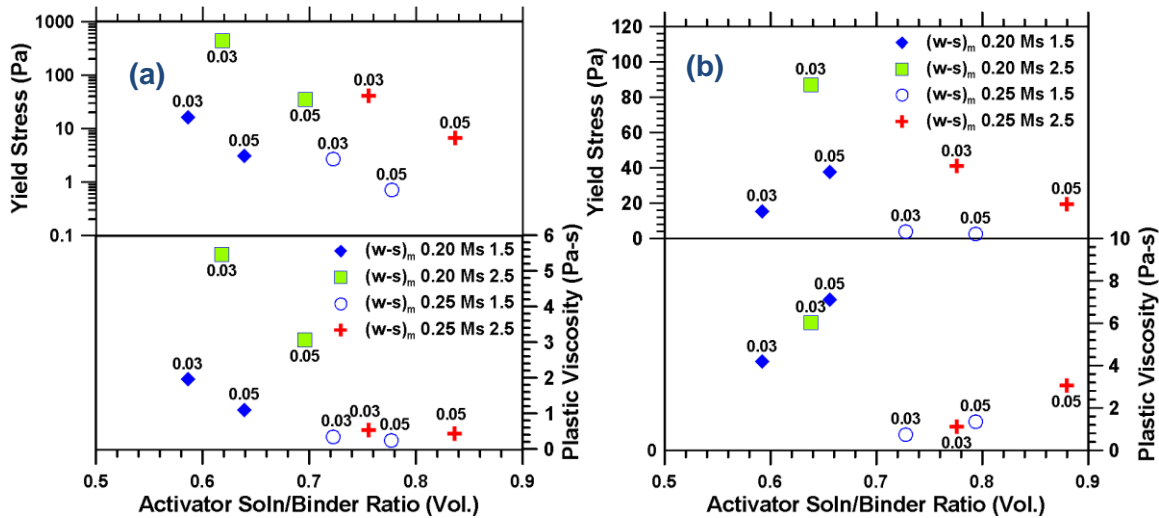
274 Several key observations are noted that are typical of these figures: (i) increasing  $M_s$  results in increases  
 275 in yield stress and plastic viscosity, (ii) a lower  $n$ -value results in more significant enhancements in yield  
 276 stress as  $M_s$  is increased, and (iii) at low values of  $M_s$  the yield stress approaches zero suggesting a  
 277 transition to Newtonian behavior. The increase in the yield stress and plastic viscosity with increasing  $M_s$   
 278 may be partially attributed to the increase in activation solution viscosity with  $M_s$  as noted in Figure 2.  
 279 The latter observations which demand careful examination are explored in the forthcoming sections.

280 When Figures 4 and 5 are compared, the following important observations can be made: (i) at a lower  
 281  $(w/s)_m$  and higher  $M_s$ , the yield stress of the fly ash-K silicate suspension is much higher than that of the  
 282 fly ash-Na silicate suspension, while the values are comparable at a higher  $(w/s)_m$ ; and (ii) increasing the  
 283  $(w/s)_m$  results in a significant reduction in plastic viscosity especially at higher  $M_s$  for the fly ash-K silicate  
 284 suspension while the reduction is much lower for the fly ash-Na silicate suspension. These observations  
 285 support the idea that flow parameters are influenced to a great extent by the adsorption of cations on  
 286 particle surfaces. At higher  $(w/s)_m$ , the surface adsorption of ions and van Der Waals forces become less  
 287 significant as the particle spacing increases, and thus the influence of the alkali cation from the activation  
 288 solution is reduced. In addition, at higher  $(w/s)_m$ , Na-based fly ash suspensions demonstrate similar or  
 289 higher yield stress as compared to K-based suspensions. Increasing the  $n$ -value is shown to decrease both

290 the yield stress and plastic viscosity in K-based suspensions, while generally increasing those values in Na-  
291 based suspensions (except for the fly ash-Na silicate suspension with an  $M_s$  of 2.5 at a  $(w/s)_m$  of 0.25). The  
292 increased rheological properties in Na silicate-fly ash suspensions as compared to K silicate-fly ash  
293 suspensions is primarily attributed to the significantly greater viscosity of the Na-based suspensions as  
294 compared to K-based suspensions as noted in Figure 2. Furthermore, in K silicate-fly ash suspensions, the  
295 behavior is Newtonian (zero yield stress) at low  $M_s$  values regardless of  $(w/s)_m$  ratio, whereas the Na-  
296 silicate suspensions exhibit the Newtonian behavior only at the higher  $(w/s)_m$ . The shift to a Newtonian  
297 flow regime at low  $M_s$  values is explored in detail in a later section.

### 298 **3.3.2 Dependence of rheological parameters on the volumetric activator solution-binder ratio**

299 The  $(w/s)_m$  ratio is a mass-based ratio of the water in the activator (along with any additional water added)  
300 to the total solids (the binder material, fly ash in this case and the solids present in any of the activating  
301 chemicals) in the suspension. The  $(a_s/b)_v$  ratio, on the other hand, is the volumetric ratio of the activation  
302 solution to the binder. The activation solution implicitly includes the dissolved solids present in the  
303 solution: both the silicate solutions used in this study have the same solids content. The use of  $(a_s/b)_v$   
304 ratio, rather than  $(w/s)_m$  (which is an easier proportioning parameter for practical applications) is deemed  
305 to be appropriate because the rheological characteristics of suspensions are typically dependent on the  
306 volume of suspending fluid present, the size, shape, and concentration of the suspended particles  
307 (Sweeny and Geckler 1954; Jeffrey and Acrivos 1976; Mueller et al. 2010; Santamaria-Holek and Mendoza  
308 2010; Bentz et al. 2012), and the rheology of the suspending medium (Krieger and Dougherty 1959; Kamal  
309 and Mutel 1985; Barnes 1989). It is further notable that the use of a constant  $(w/s)_m$  while modifying the  
310  $n$  and  $M_s$  values will not result in a constant  $(a_s/b)_v$  due to the influence of changing amounts of MOH  
311 added to the activator solution to maintain the desired  $M_s$ . Generally, increasing either  $M_s$  or  $n$  will  
312 increase the  $(a_s/b)_v$  ratio due to an increase in solids present in the activator, requiring an increase in  
313 solution volume to maintain a constant  $(w/s)_m$  ratio. Thus, at the same  $(w/s)_m$  ratio, an activation solution  
314 with a higher  $n$  and/or  $M_s$  will have both a higher  $(a_s/b)_v$  ratio and a higher added  $M^+$  ion concentration.

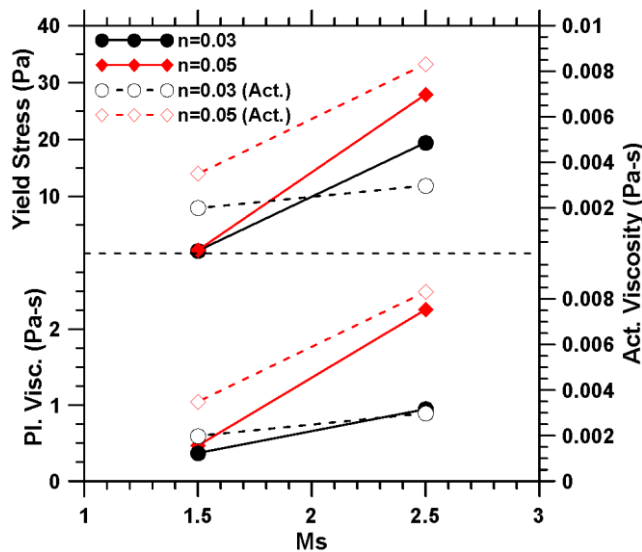


315  
 316 **Fig. 6** Influence of  $(a_s/b)_v$  ratio on rheological properties for: (a) fly ash-K silicate suspensions, and (b) fly  
 317 ash-Na silicate suspensions (labels in parentheses are the n-values).

318 Figures 6(a) and (b) illustrate the influence of  $(a_s/b)_v$  on the yield stress and plastic viscosity of Na- and K-  
 319 silicate activated fly ash suspensions respectively. In general, the yield stress and the plastic viscosity  
 320 decrease for all the suspensions as the  $(a_s/b)_v$  increases, due to the reduction in particle concentration.  
 321 This is a trend that is expected, as in the case of OPC when the  $(w/p)_v$  is increased (Ferraris 1999). For both  
 322 K- and Na-based suspensions, with an increase in  $M_s$ , at the same n value, it is observed that both the  
 323 yield stress and plastic viscosity increases. One can also notice that, for the same n value, the  $(a_s/b)_v$  is  
 324 higher at a higher  $M_s$ , while in most cases rheological parameters increase despite this fact, indicating  
 325 other underlying phenomena, which will be discussed later. At the same  $(w/s)_m$  and  $M_s$ , the rheological  
 326 parameters decrease with an increase in n, which is attributable to the increased amount of MOH solution  
 327 added to increase n, and the consequent reduction in the volume fraction of solids provided by the  
 328 activator. The only exception is the Na silicate-fly ash suspension at an  $M_s$  of 1.5 and  $(w/s)_m$  of 0.20 ( $a_s/b$   
 329 of 0.66) where an increase in n increases both the yield stress and plastic viscosity despite the fact that  
 330 increasing n results in an increase in the volume of activator solution. This inconsistency is attributed to  
 331 more significant changes in the Na-based activator solution viscosity as noted previously in Figure 2.  
 332 Further, the increase in plastic viscosity with increasing  $(a_s/b)_v$  in Na-silicate fly ash suspensions could have  
 333 been augmented by the higher concentration of  $Na^+$  present which decreases the absolute surface charge  
 334 of fly ash and thus the steric forces.

335 To further investigate possible influences in these suspensions, and disconnect the influence of solids  
 336 content provided by the activator on the rheological parameters, suspensions of fly ash in potassium  
 337 silicate activator solutions were prepared where a constant  $(a_s/b)_v$  ratio of 0.72 was maintained while

338 varying  $M_s$  and  $n$ . The results are presented in Figure 8 which shows the yield stress and plastic viscosity  
 339 of the suspensions and the activation solution viscosity as a function of  $M_s$ . Similar trends as in Figure 4  
 340 are noted, where increasing  $M_s$  results in increased yield stress and plastic viscosity. However, at a  
 341 constant  $(a_s/b)_v$ , increasing  $n$  increases both yield stress and plastic viscosity, especially at the higher  $M_s$   
 342 value. This is opposite to what was observed in Figure 6(a) where the influence of  $n$  and  $(a_s/b)_v$  were  
 343 confounded. It is noted from this figure that there is a strong correlation between the trends of activation  
 344 solution viscosity and the plastic viscosity of the resultant suspension. This indicates that the dominant  
 345 influence on the suspension viscosity is the viscosity of the suspending solution itself and the solids  
 346 loading. Yield stress is also found to demonstrate similar trends as the activation solution viscosity when  
 347 plotted as a function of  $M_s$ , for the suspension with an  $n$  value of 0.05. However, at an  $n$  value of 0.03, the  
 348 activation solution viscosity barely changes with  $M_s$  whereas the yield stress increase is significant. It can  
 349 thus be postulated with reasonable certainty that the activation solution viscosity is a less dominant  
 350 influence on yield stress. Yield stress of activated fly ash suspensions is thus dominated by influences of  
 351 solid loading and particle interactions as is the general case for particulate suspensions, while the plastic  
 352 viscosity is more strongly influenced by activation solution viscosity and solids loading.



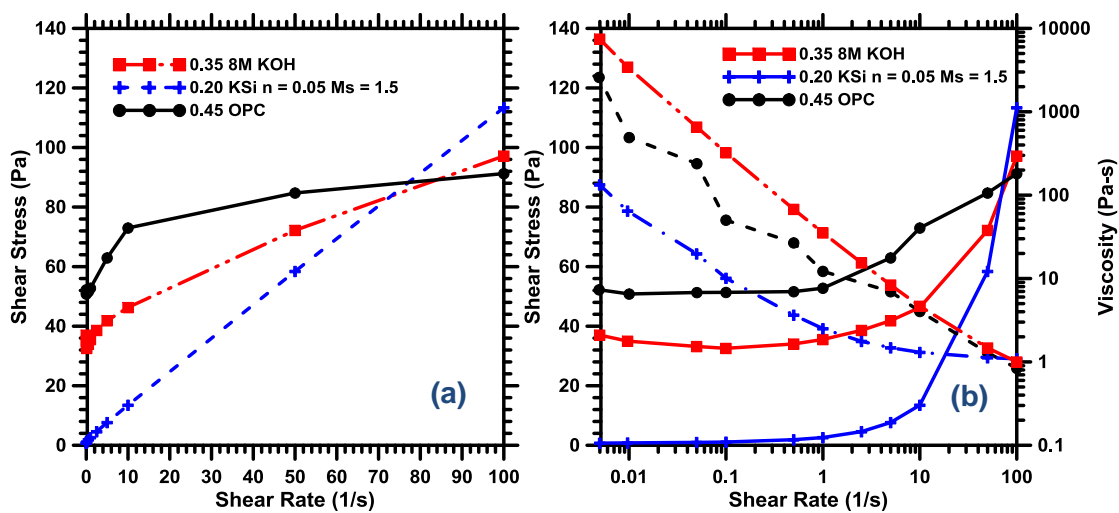
353

354 **Fig. 7** Investigation of influence of  $n$  and  $M_s$  at a constant  $(a_s/b)_v$  ratio of 0.72. Solid lines represent the  
 355 determined suspension rheological parameters, dashed lines represent rheological properties of  
 356 activation solution.

### 357 3.4 Rheological Response of Suspensions under Extended Shear Rates

#### 358 3.4.1 Comparison of Activated Fly ash Suspensions to OPC-Water Suspensions

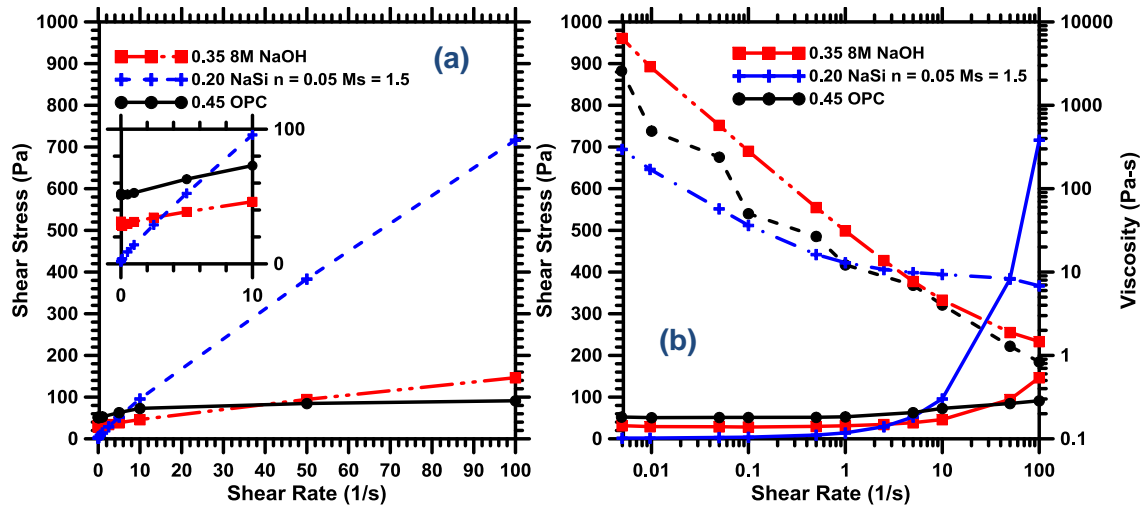
359 The purpose of this section is to investigate the differences and/or similarities in rheological behavior of  
 360 suspensions of fly ash particles in an alkaline activator to ordinary portland cement (OPC) particles in  
 361 water. The experiments for this study, including that for the Type I/II OPC suspension were completed  
 362 using the “wide” rheological procedure as presented in Section 2. This procedure allows for a model-less  
 363 estimation of apparent yield stress (Barnes 1999; Vance et al. 2013) based on the stress plateau that is  
 364 not discerned in the typical shear rate ranges employed in rheological studies of cementitious systems  
 365 (Vance, Kirk 2014). Figures 8 and 9 present the flow (shear stress-shear rate) curves plotted in both linear  
 366 and logarithmic scales to allow for more in-depth discussion of the rheological response of these  
 367 suspensions. Solid loading in the various suspensions was adjusted so as to achieve flow curves that were  
 368 roughly in the same shear stress range over the range of shear rates investigated (in a strain rate range of  
 369 5-100/s that is used in conventional rheological studies of cementitious suspensions) to facilitate  
 370 comparison.



371

372 **Fig. 8** Comparison of rheological response of fly ash suspensions in KOH and K-silicate solutions and  
 373 portland cement-water suspension: (a) shear stress response in linear scale and (b) shear stress (solid)  
 374 and viscosity response (dashed) in logarithmic scale





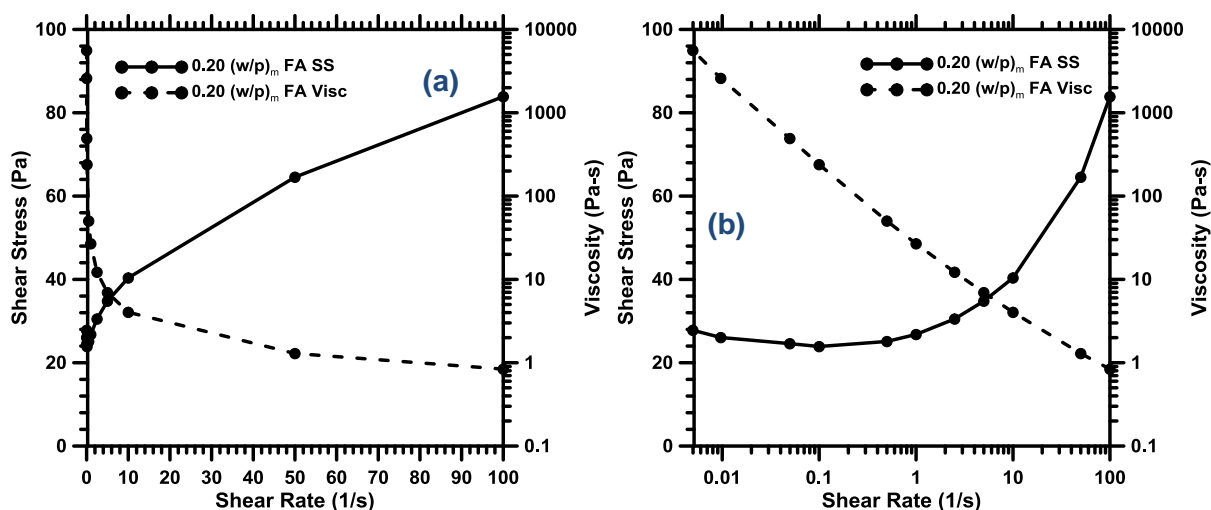
375

376 **Fig. 9** Comparison of rheological response of fly ash suspensions in NaOH and Na-silicate solutions and  
 377 portland cement-water suspension: (a) shear stress response in linear scale and (b) shear stress (solid)  
 378 and viscosity (dashed) response in logarithmic scale

379 It is evident from Figures 8 and 9 that the general shear rate-shear stress response of the fly ash-MOH  
 380 suspensions is quite similar to that of the portland cement-water suspension. In both cases there is a  
 381 stress plateau at lower shear rates ( $< 1/s$ ) indicating an apparent yield stress (Cheng 1986; Barnes 1999),  
 382 which is preceded by a linear portion at relatively constant slope from shear rates of about 10 to 100/s.  
 383 In the linear scale, both KOH and NaOH based suspensions show the typical downward trend at low shear  
 384 rates that has been documented in several other publications of cementitious material rheology (Atzeni  
 385 et al. 1985; Vance et al. 2013). In the KOH-fly ash suspension, there is a noted upward trend in shear stress  
 386 at the very low end of shear rates along the stress plateau region. This is indicative of flow instabilities  
 387 associated with localized particle diffusion and reorganization (Schall and van Hecke 2009). As shear is  
 388 applied to a suspension, localized particle rearrangement occur to enable flow, at very low shear rates,  
 389 when there is insufficient strain to maintain, this localized reordering is destroyed and an instability in the  
 390 flow curve results. The existence of the this trend in K-based suspensions and its absence in Na-based  
 391 suspensions supports the presence of a higher surface charge on fly ash particles in K-based suspensions  
 392 as compared to Na-based suspensions. This higher surface charge promotes the fly ash particles to move  
 393 into the less concentrated region and to a less organized state to achieve a state of minimized energy (i.e.,  
 394 minimized interparticle repulsion), which results in an increased resistance to flow of the suspension  
 395 indicated by an increase in stress (Callaghan 2008; Schall and van Hecke 2009).

396 **3.4.2 Discussions on the changes in rheological response with activator  $M_s$**

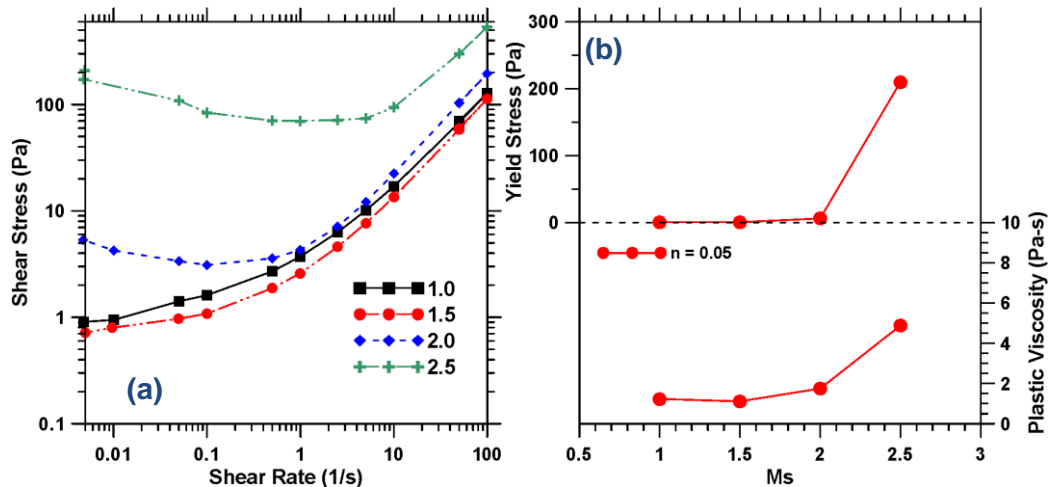
397 The behavior of the silicate based activator suspensions is noted to be quite different as compared to the  
 398 MOH activated systems. While the OPC and hydroxide-based suspensions demonstrate a viscosity range  
 399 of about 4 orders of magnitude from the highest to lowest shear rate, the viscosity of the silicate based  
 400 suspensions only increases by 2 orders of magnitude over the same shear rate range, as noted in Figures  
 401 8(b) and 9(b). Further, on a log scale, the viscosity-shear rate relationships of the OPC-water and fly ash-  
 402 MOH suspensions appears linear; while the silicate based suspensions demonstrate a viscosity asymptote  
 403 at higher shear rates. To investigate the cause of this behavior, additional experiments were conducted  
 404 using a mixture of fly ash and water with the same mass-based liquid to powder ratio as used in the silicate  
 405 based activator experiments as shown in Figure 10.



406  
 407 **Fig. 10** Rheological study of 0.20 (w/s)<sub>m</sub> suspension of fly ash and water: (a) linear scale and (b)  
 408 logarithmic scale. Shear stress (solid) and viscosity (dashed).

409 The fly ash-water suspension shows rheological behavior that bears more resemblance to that of the fly  
 410 ash-MOH or OPC-water suspensions. In this case, a noted stress plateau and an increase in viscosity by  
 411 almost 4 orders of magnitude over the range of shear rates investigated are observed. Given that the  
 412 activation solutions in these suspensions have viscosities of 0.0017 and 0.0054 Pa-s (Figure 2) for  
 413 potassium silicate and sodium silicate respectively, which are meaningfully greater than that of water  
 414 (approximately 0.00089 Pa-s at 25 °C), this behavior is counterintuitive. It can be noted from Figures 4  
 415 and 5 that at higher values of  $M_s$ , in all suspensions investigated, the existence of an apparent yield stress  
 416 is observed; i.e., the fly ash suspensions employing activators of higher  $M_s$  are non-Newtonian. As the  
 417 Newtonian behavior is not present in fly ash-water suspensions, and it disappears at a higher value of  $M_s$ ,  
 418 this indicates a clear influence of the siliceous species and the free  $M^+$  ion concentration present in the  
 419 suspension. To better understand this, additional experiments were conducted at  $M_s$  values of 1.0 and 2.0

420 to investigate the range in which this phenomenon is present, as presented in Figure 11. At low  $M_s$  values  
 421 (1.0 and 1.5), the Newtonian shift is visible with the absence of a stress plateau in Figure 11(a), while at  
 422 larger  $M_s$  values, the behavior transitions to non-Newtonian as a stress plateau is formed. It is possible  
 423 that the increased quantity of hydroxide ions present in the solutions at lower values of  $M_s$ , results in a  
 424 decreased polymerization of the colloidal silica species as discussed previously. This in turn results in  
 425 colloidal species that may act in a fashion similar to superplasticizers in cement. When superplasticizers  
 426 are added to portland cement suspensions, the suspension transitions to shear thickening as indicated by  
 427 an upward trend in the viscosity-shear rate plot. Fly ash suspensions in silica based activators indicate a  
 428 shift towards shear-thickening behavior in Figures 8 and 9 as indicated by the significant decrease in  
 429 magnitude of viscosity reduction over the range of shear rates studied (Lootens et al. 2004; Papo and Piani  
 430 2004).

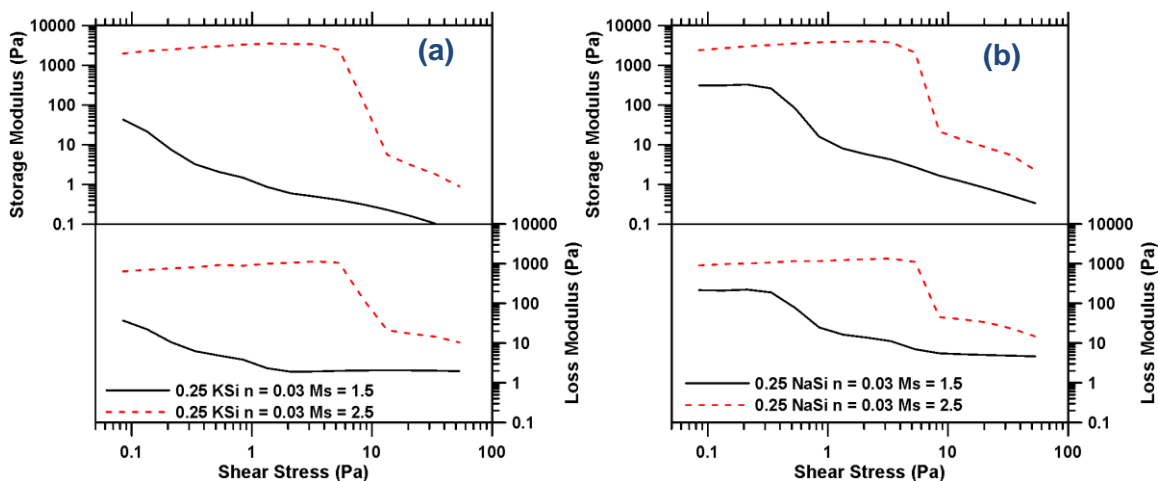


431  
 432 **Fig. 11** – Rheological study of 0.25 (w/s)<sub>m</sub> K-Si fly ash suspension at varying  $M_s$ : (a) flow curve in  
 433 logarithmic scale and (b) influence of  $M_s$  on determined rheological properties

434 **3.4.3 Response at different activator  $M_s$ : Shear stress growth experiments**

435 A small amplitude oscillatory shear stress growth experiment was carried out on the fly ash - silicate  
 436 suspensions corresponding to a (w/s)<sub>m</sub> of 0.25. The results of this experiment are presented in Figure 12  
 437 which also shows the influence of reducing  $M_s$  on the rheological behavior of the system. Noted from this  
 438 figure is the significant change in behavior for the suspensions at a low  $M_s$  with respect to both the storage  
 439 and loss moduli. The storage modulus ( $G'$ ) and loss modulus ( $G''$ ) are related to the elastic and viscous  
 440 portions of a viscoelastic material respectively (Barnes et al. 2000; Nehdi and Rahman 2004). The expected  
 441 trend in cementitious suspensions is a plateau region at low stress indicative of the linear viscoelastic  
 442 region, followed by a significant decrease in both the storage and loss moduli at higher stresses, which

443 indicates structural breakdown of the suspension (Nehdi and Rahman 2004). This low stress plateau is  
 444 noted in all suspensions investigated except the K-Si suspension at an  $M_s$  of 1.5, which is likely present at  
 445 a further lower stress than that investigated in this study. Performing this experiment at further lower  
 446 stresses resulted in increased data scatter due to the fact that the measured stresses were nearing the  
 447 torque limit of the instrument, and hence they are not presented here. At lower  $M_s$  values, the critical  
 448 linear viscoelastic stress is shifted drastically to the left, and the height of the plateau region is an order  
 449 of magnitude lower. The significantly higher storage modulus for the higher activator  $M_s$  suspension  
 450 indicates a more structurally organized system, which supports the observations and explanations  
 451 discussed earlier. At an  $M_s$  value of 1.5 there is a change in behavior of the suspension, possibly attributed  
 452 to the charged colloidal siliceous species present in this system, or surface charge effects on the fly ash  
 453 particles. Further, the drastic decrease in magnitude of the stress plateau and leftward shift of the critical  
 454 linear viscoelastic stress is indicative of a behavior similar to that observed in OPC suspensions in the  
 455 presence of high-range water reducing admixtures (Nehdi and Rahman 2004). A lower stress plateau is  
 456 indicative of well-dispersed particles in a suspension with a less defined networked structure, likely caused  
 457 by increased repulsive forces between fly ash particles. The exact nature of these phenomena requires  
 458 future investigation, particularly in the context of understanding the solution chemistry of the alkali-  
 459 silicate activator solutions. Given the noted inconsistencies in the use of superplasticizers in geopolymer  
 460 suspensions (Palacios et al. 2009), an understanding of this phenomena may allow for optimization of the  
 461 flow properties of geopolymer concretes without the use of chemical admixtures.



462  
 463 **Fig. 12** Oscillatory shear study of 0.25 (w/s)<sub>m</sub> fly ash suspensions with (a) K-Si based activator, and (b)  
 464 Na-Si based activator

465 **4.0 CONCLUSIONS**

466 The influence of activator type and concentration on the rheological characteristics of fly ash suspension  
467 is reported. Hydroxides and silicates of Na and K were used as the activation solutions, the viscosities of  
468 which increased with molarity (for hydroxides) or  $M_s$  (for silicates), with the Na-based activators  
469 demonstrating higher viscosities than their k-based counterparts. The rheological properties of NaOH or  
470 KOH activated fly ash were found to be primarily influenced by the changes in the viscosity of the  
471 suspending fluid and surface charge of the fly ash particles. Na-based suspensions demonstrated a large  
472 increase in viscosity due to the more significant increase in the viscosity of the suspending fluid while K-  
473 based suspensions showed a more significant increase in yield stress, attributed to the greater adsorption  
474 of less well hydrated  $K^+$  ions onto the surface of the fly ash particles, reducing the repulsive effect between  
475 fly ash particles.

476 The rheological response of fly ash-alkali silicate suspensions were found to be complex. The yield stress  
477 and plastic viscosity of suspensions were observed to increase with  $M_s$  with the yield stress tending to  
478 zero (i.e., approaching Newtonian behavior) at low activator  $M_s$  values. Increasing the water-to-solids  
479 ratio and/or the  $n$  value of the suspension resulted in significantly different yield stress and plastic  
480 viscosity trends for the Na- and K-based suspensions, pointing to the influence of both the activation  
481 solution viscosity and cationic adsorption on the fly ash particle surfaces that greatly influence the  
482 suspension rheology. Experiments on suspensions with controlled activation solution-to-binder ratios  
483 (volume-basis) showed the influence of several key parameters on the rheological properties. The plastic  
484 viscosity was found to be influenced strongly by the solid loading and the activation solution viscosity,  
485 while yield stress appears to be less influenced by activation solution viscosity and more strongly  
486 influenced by interaction effects produced by the surface charges on the fly ash particles, which are  
487 dependent on the cationic type.

488 In silicate based suspensions, for low  $M_s$ , the suspension demonstrated a transition to a Newtonian  
489 behavior, with a zero yield stress. While the OPC and hydroxide-based suspensions demonstrated a  
490 viscosity range of about 4 orders of magnitude from the highest to lowest shear rate (100/s to 0.005/s),  
491 the viscosity of the silicate based suspensions increased by only 2 orders of magnitude over the same  
492 shear rate range. The fly ash-water suspension also behaved similar to the OPC-water and fly ash-MOH  
493 suspensions. A small amplitude oscillatory stress growth experiment showed that the critical linear  
494 viscoelastic stress plateau shifts to much lower shear stress ranges, and the storage/loss moduli reduces  
495 at lower  $M_s$  values, akin to the response of superplasticized cementitious suspensions. The exact nature  
496 of this transition is not fully understood and requires additional work.

## 497 **5.0 ACKNOWLEDGEMENTS**

498 The authors gratefully acknowledge the National Science Foundation (CMMI 1068985) and Arizona State  
499 University for the partial support of this research. The materials for this research were provided by  
500 Headwaters Resources and PQ Corporation, and are acknowledged. K.V. also acknowledges the Dean's  
501 Fellowship from the Ira A. Fulton Schools of Engineering at Arizona State University (ASU). This research  
502 was conducted in the Laboratory for the Science of Sustainable Infrastructural Materials (LS-SIM) at ASU  
503 and the authors gratefully acknowledge the support that has made this laboratory possible. The contents  
504 of this paper reflect the views of the authors who are responsible for the facts and accuracy of the data  
505 presented herein, and do not necessarily reflect the views and policies of the funding agency, nor do the  
506 contents constitute a standard, specification, or a regulation.

## 507 **BIBLIOGRAPHY**

- 508 Atzeni C, Massidda L, Sanna U (1985) Comparison between rheological models for portland cement  
509 pastes. *Cem Concr Res* 15:511–519. doi: 16/0008-8846(85)90125-5
- 510 Banfill PFG (2006) Rheology of fresh cement and concrete. *Rheol Rev* 2006:61.
- 511 Barnes HA (1999) The yield stress—a review or “ $\pi\alpha\nu\tau\alpha \rho\epsilon\varsigma\iota\alpha\varsigma$ ”—everything flows? *J Non-Newton*  
512 *Fluid Mech* 81:133–178.
- 513 Barnes HA (1989) Shear-thickening (“dilatancy”) in suspensions of nonaggregating solid particles  
514 dispersed in Newtonian liquids. *J Rheol* 33:329.
- 515 Barnes HA, Non-Newtonian I of, Mechanics F (2000) A handbook of elementary rheology. Univ. of  
516 Wales, Institute of Non-Newtonian Fluid Mechanics
- 517 Bentz DP, Ferraris CF, Galler MA, et al. (2012) Influence of particle size distributions on yield stress and  
518 viscosity of cement–fly ash pastes. *Cem. Concr. Res.*
- 519 Bernal SA, Mejía de Gutiérrez R, Provis JL (2012) Engineering and durability properties of concretes  
520 based on alkali-activated granulated blast furnace slag/metakaolin blends. *Constr Build Mater*  
521 33:99–108.
- 522 Bijen J (1996) Benefits of slag and fly ash. *Constr Build Mater* 10:309–314.
- 523 Bingham EC (1922) Fluidity and plasticity.
- 524 Brady JF (1993) The rheological behavior of concentrated colloidal dispersions. *J Chem Phys* 99:567–581.
- 525 Burgos-Montes O, Palacios M, Rivilla P, Puertas F (2012) Compatibility between superplasticizer  
526 admixtures and cements with mineral additions. *Constr Build Mater* 31:300–309.
- 527 Callaghan PT (2008) Rheo NMR and shear banding. *Rheol Acta* 47:243–255.
- 528 Cheng DC-H (1986) Yield stress: A time-dependent property and how to measure it. *Rheol Acta* 25:542–  
529 554. doi: 10.1007/BF01774406

- 530 Criado M, Palomo A, Fernández-Jiménez A, Banfill PFG (2009) Alkali activated fly ash: effect of  
531 admixtures on paste rheology. *Rheol Acta* 48:447–455.
- 532 Cyr M, Legrand C, Mouret M (2000) Study of the shear thickening effect of superplasticizers on the  
533 rheological behaviour of cement pastes containing or not mineral additives. *Cem Concr Res*  
534 30:1477–1483. doi: 10.1016/S0008-8846(00)00330-6
- 535 Davidovits J (1999) Chemistry of geopolymeric systems, terminology. *Geopolymer*. pp 9–40
- 536 Davidovits J (2005) Geopolymer chemistry and sustainable development. The poly (sialate) terminology:  
537 a very useful and simple model for the promotion and understanding of green-chemistry. *Proc.*  
538 2005 Geopolymer Conf. pp 9–15
- 539 Fernández-Jiménez A, Garcia-Lodeiro I, Palomo A (2007) Durability of alkali-activated fly ash  
540 cementitious materials. *J Mater Sci* 42:3055–3065.
- 541 Ferraris CF (1999) Measurement of the rheological properties of high performance concrete: state of the  
542 art report. *J Res-Natl Inst Stand Technol* 104:461–478.
- 543 Franks GV (2002) Zeta potentials and yield stresses of silica suspensions in concentrated monovalent  
544 electrolytes: isoelectric point shift and additional attraction. *J Colloid Interface Sci* 249:44–51.
- 545 Iler RK (1979) The chemistry of silica: solubility, polymerization, colloid and surface properties, and  
546 biochemistry.
- 547 Jeffrey DJ, Acrivos A (1976) The rheological properties of suspensions of rigid particles. *AIChE J* 22:417–  
548 432.
- 549 Kamal MR, Mutel A (1985) Rheological Properties of Suspensions in Newtonian and Non-Newtonian  
550 Fluids. *J Polym Eng* 5:293–382. doi: 10.1515/POLYENG.1985.5.4.293
- 551 Krieger IM, Dougherty TJ (1959) A mechanism for non-Newtonian flow in suspensions of rigid spheres.  
552 *Trans Soc Rheol* 3:137–152.
- 553 Lootens D, Hébraud P, Lécolier E, Van Damme H (2004) Gelation, shear-thinning and shear-thickening in  
554 cement slurries. *Oil Gas Sci Technol* 59:31–40.
- 555 Lowke D (2009) *Interparticle Forces and Rheology of Cement Based Suspensions*. Nanotechnol. Constr.  
556 3. Springer, pp 295–301
- 557 Mannheimer RJ (1983) Effect Of Slip On The Flow Properties Of Cement Slurries. *Annu. Meet. Pap. Div.*  
558 *Prod.*
- 559 Mikanovic N, Jolicoeur C (2008) Influence of superplasticizers on the rheology and stability of limestone  
560 and cement pastes. *Cem Concr Res* 38:907–919.
- 561 Mueller S, Llewellyn EW, Mader HM (2010) The rheology of suspensions of solid particles. *Proc R Soc*  
562 *Math Phys Eng Sci* 466:1201–1228. doi: 10.1098/rspa.2009.0445

- 563 Nägele E (1986) The Zeta-potential of cement: Part II: Effect of pH-value. *Cem Concr Res* 16:853–863.
- 564 Nägele E, Schneider U (1989) The zeta-potential of blast furnace slag and fly ash. *Cem Concr Res* 19:811–  
565 820.
- 566 Nehdi M, Rahman M-A (2004) Effect of geometry and surface friction of test accessory on oscillatory  
567 rheological properties of cement pastes. *ACI Mater. J.* 101:
- 568 Palacios M, Houst YF, Bowen P, Puertas F (2009) Adsorption of superplasticizer admixtures on alkali-  
569 activated slag pastes. *Cem Concr Res* 39:670–677.
- 570 Palomo A, Grutzeck MW, Blanco MT (1999) Alkali-activated fly ashes: a cement for the future. *Cem*  
571 *Concr Res* 29:1323–1329.
- 572 Papo A, Piani L (2004) Effect of various superplasticizers on the rheological properties of Portland  
573 cement pastes. *Cem Concr Res* 34:2097–2101.
- 574 Pasquino R, Nicodemi F, Vanzanella V, et al. (2013) A rheological phase diagram of additives for cement  
575 formulations. *Rheol Acta* 52:395–401.
- 576 Poulesquen A, Frizon F, Lambertin D (2013) Rheological behavior of alkali-activated metakaolin during  
577 geopolymerization. *Cem.-Based Mater. Nucl. Waste Storage*. Springer, pp 225–238
- 578 Provis JL, Muntingh Y, Lloyd RR, et al. (2007) Will Geopolymers Stand the Test of Time? *Dev Porous Biol*  
579 *Geopolymer Ceram Ceram Eng Sci Proc* 235.
- 580 Provis JL, Van Deventer JSJ (2009) *Geopolymers: structure, processing, properties and industrial*  
581 *applications*. Woodhead Cambridge, UK
- 582 Puertas F, Fernández-Jiménez A (2003) Mineralogical and microstructural characterisation of alkali-  
583 activated fly ash/slag pastes. *Cem Concr Compos* 25:287–292.
- 584 Qing-Hua C, Sarkar SL (1994) A study of rheological and mechanical properties of mixed alkali activated  
585 slag pastes. *Adv Cem Based Mater* 1:178–184.
- 586 Ravikumar D, Neithalath N (2012b) Reaction kinetics in sodium silicate powder and liquid activated slag  
587 binders evaluated using isothermal calorimetry. *Thermochim. Acta*
- 588 Ravikumar D, Neithalath N (2012a) Effects of activator characteristics on the reaction product formation  
589 in slag binders activated using alkali silicate powder and NaOH. *Cem Concr Compos* 34:809–818.  
590 doi: 10.1016/j.cemconcomp.2012.03.006
- 591 Saak AW, Jennings HM, Shah SP (2001) The influence of wall slip on yield stress and viscoelastic  
592 measurements of cement paste. *Cem Concr Res* 31:205–212.
- 593 Santamaria-Holek I, Mendoza CI (2010) The rheology of concentrated suspensions of arbitrarily-shaped  
594 particles. *ArXiv10055707 Cond-Mat*



- 595 Scales PJ, Johnson SB, Healy TW, Kapur PC (1998) Shear yield stress of partially flocculated colloidal  
596 suspensions. *AIChE J* 44:538–544.
- 597 Schall P, van Hecke M (2009) Shear bands in matter with granularity. *Annu Rev Fluid Mech* 42:67.
- 598 Škvára F, Kopecký L, Šmilauer V, Bittnar Z (2009) Material and structural characterization of alkali  
599 activated low-calcium brown coal fly ash. *J Hazard Mater* 168:711–720. doi:  
600 10.1016/j.jhazmat.2009.02.089
- 601 Stebbins JF, Farnan I, Xue X (1992) The structure and dynamics of alkali silicate liquids: A view from NMR  
602 spectroscopy. *Chem Geol* 96:371–385.
- 603 Svensson IL, Sjöberg S, Öhman L-O (1986) Polysilicate equilibria in concentrated sodium silicate  
604 solutions. *J Chem Soc Faraday Trans 1* 82:3635–3646.
- 605 Sweeny KH, Geckler RD (1954) The Rheology of Suspensions. *J Appl Phys* 25:1135–1144. doi:  
606 doi:10.1063/1.1721828
- 607 Termkhajornkit P, Nawa T (2004) The fluidity of fly ash–cement paste containing naphthalene sulfonate  
608 superplasticizer. *Cem Concr Res* 34:1017–1024.
- 609 Tognonvi MT, Massiot D, Lecomte A, et al. (2010) Identification of solvated species present in  
610 concentrated and dilute sodium silicate solutions by combined <sup>29</sup>Si NMR and  
611 SAXS studies. *J Colloid Interface Sci* 352:309–315.
- 612 Vance K, Kumar A, Sant G, Neithalath N (2013) The rheological properties of ternary binders containing  
613 Portland cement, limestone, and metakaolin or fly ash. *Cem Concr Res* 52:196–207. doi:  
614 10.1016/j.cemconres.2013.07.007
- 615 Vance, Kirk (2014) Early Age Characterization and Microstructural Features of Sustainable Binder  
616 Systems for Concrete. PhD Dissertation, Arizona State University
- 617 Wijnen P, Beelen TPM, De Haan JW, et al. (1989) Silica gel dissolution in aqueous alkali metal hydroxides  
618 studied by <sup>29</sup>Si NMR. *J Non-Cryst Solids* 109:85–94.
- 619 (2013) ASTM C109-13. Standard Test Method for Compressive Strength of Hydraulic Cement Mortars  
620 Using 2-in. Cube Specimens.
- 621 (2011) ASTM C1738 - 11a. Standard Practice for High-Shear Mixing of Hydraulic Cement Paste.
- 622